

Measurement of the absolute branching fraction of $\Lambda_c^+ \rightarrow pK_S^0\eta$ decays

M. Ablikim¹, M. N. Achasov^{10,c}, P. Adlarson⁶⁴, S. Ahmed¹⁵, M. Albrecht⁴, R. Aliberti²⁸, A. Amoroso^{63A,63C}, Q. An^{60,48}, Anita²¹, X. H. Bai⁵⁴, Y. Bai⁴⁷, O. Bakina²⁹, R. Baldini Ferroli^{23A}, I. Balossino^{24A}, Y. Ban^{38,k}, K. Begzsuren²⁶, J. V. Bennett⁵, N. Berger²⁸, M. Bertani^{23A}, D. Bettoni^{24A}, F. Bianchi^{63A,63C}, J. Biernat⁶⁴, J. Bloms⁵⁷, A. Bortone^{63A,63C}, I. Boyko²⁹, R. A. Briere⁵, H. Cai⁶⁵, X. Cai^{1,48}, A. Calcaterra^{23A}, G. F. Cao^{1,52}, N. Cao^{1,52}, S. A. Cetin^{51B}, J. F. Chang^{1,48}, W. L. Chang^{1,52}, G. Chelkov^{29,b}, D. Y. Chen⁶, G. Chen¹, H. S. Chen^{1,52}, M. L. Chen^{1,48}, S. J. Chen³⁶, X. R. Chen²⁵, Y. B. Chen^{1,48}, Z. J. Chen^{20,l}, W. S. Cheng^{63C}, G. Cibinetto^{24A}, F. Cossio^{63C}, X. F. Cui³⁷, H. L. Dai^{1,48}, J. P. Dai^{42,g}, X. C. Dai^{1,52}, A. Dbeyssi¹⁵, R. B. de Boer⁴, D. Dedovich²⁹, Z. Y. Deng¹, A. Denig²⁸, I. Denysenko²⁹, M. Destefanis^{63A,63C}, F. De Mori^{63A,63C}, Y. Ding³⁴, C. Dong³⁷, J. Dong^{1,48}, L. Y. Dong^{1,52}, M. Y. Dong^{1,48,52}, S. X. Du⁶⁸, J. Fang^{1,48}, S. S. Fang^{1,52}, Y. Fang¹, R. Farinelli^{24A}, L. Fava^{63B,63C}, F. Feldbauer⁴, G. Felici^{23A}, C. Q. Feng^{60,48}, M. Fritsch⁴, C. D. Fu¹, Y. Fu¹, X. L. Gao^{60,48}, Y. Gao^{38,k}, Y. Gao⁶¹, Y. G. Gao⁶, I. Garzia^{24A,24B}, E. M. Gersabeck⁵⁵, A. Gilman⁵⁶, K. Goetzen¹¹, L. Gong³⁷, W. X. Gong^{1,48}, W. Gradl²⁸, M. Greco^{63A,63C}, L. M. Gu³⁶, M. H. Gu^{1,48}, S. Gu², Y. T. Gu¹³, C. Y. Guan^{1,52}, A. Q. Guo²², L. B. Guo³⁵, R. P. Guo⁴⁰, Y. P. Guo^{9,h}, Y. P. Guo²⁸, A. Guskov²⁹, S. Han⁶⁵, T. T. Han⁴¹, T. Z. Han^{9,h}, X. Q. Hao¹⁶, F. A. Harris⁵³, K. L. He^{1,52}, F. H. Heinsius⁴, C. H. Heinz²⁸, T. Held⁴, Y. K. Heng^{1,48,52}, M. Himmelreich^{11,f}, T. Holtmann⁴, Y. R. Hou⁵², Z. L. Hou¹, H. M. Hu^{1,52}, J. F. Hu^{42,g}, T. Hu^{1,48,52}, Y. Hu¹, G. S. Huang^{60,48}, L. Q. Huang⁶¹, X. T. Huang⁴¹, Y. P. Huang¹, Z. Huang^{38,k}, N. Huesken⁵⁷, T. Hussain⁶², W. Ikegami Andersson⁶⁴, W. Imoehl²², M. Irshad^{60,48}, S. Jaeger⁴, S. Janchiv^{26,j}, Q. Ji¹, Q. P. Ji¹⁶, X. B. Ji^{1,52}, X. L. Ji^{1,48}, H. B. Jiang⁴¹, X. S. Jiang^{1,48,52}, X. Y. Jiang³⁷, J. B. Jiao⁴¹, Z. Jiao¹⁸, S. Jin³⁶, Y. Jin⁵⁴, T. Johansson⁶⁴, N. Kalantar-Nayestanaki³¹, X. S. Kang³⁴, R. Kappert³¹, M. Kavatsyuk³¹, B. C. Ke^{43,1}, I. K. Keshk⁴, A. Khoukaz⁵⁷, P. Kiese²⁸, R. Kiuchi¹, R. Kliemt¹¹, L. Koch³⁰, O. B. Kolcu^{51B,e}, B. Kopf⁴, M. Kuemmel⁴, M. Kuessner⁴, A. Kupsch⁶⁴, M. G. Kurth^{1,52}, W. Kühn³⁰, J. J. Lane⁵⁵, J. S. Lange³⁰, P. Larin¹⁸, L. Lavezzi^{63A,63C}, H. Leithoff²⁸, M. Lellmann²⁸, T. Lenz²⁸, C. Li³⁹, C. H. Li³³, Cheng Li^{60,48}, D. M. Li⁶⁸, F. Li^{1,48}, G. Li¹, H. Li⁴³, H. B. Li^{1,52}, H. J. Li^{9,h}, J. L. Li⁴¹, J. Q. Li⁴, Ke Li¹, L. K. Li¹, Lei Li³, P. L. Li^{60,48}, P. R. Li³², S. Y. Li⁵⁰, W. D. Li^{1,52}, W. G. Li¹, X. H. Li^{60,48}, X. L. Li⁴¹, Z. B. Li⁴⁹, Z. Y. Li⁴⁹, H. Liang^{60,48}, H. Liang^{1,52}, Y. F. Liang⁴⁵, Y. T. Liang²⁵, L. Z. Liao^{1,52}, J. Libby²¹, C. X. Lin⁴⁹, B. Liu^{42,g}, B. J. Liu¹, C. X. Liu¹, D. Liu^{60,48}, D. Y. Liu^{42,g}, F. H. Liu⁴⁴, Fang Liu¹, Feng Liu⁶, H. B. Liu¹³, H. M. Liu^{1,52}, Huanhuan Liu¹, Huihui Liu¹⁷, J. B. Liu^{60,48}, J. Y. Liu^{1,52}, K. Liu¹, K. Y. Liu³⁴, Ke Liu⁶, L. Liu^{60,48}, Q. Liu⁵², S. B. Liu^{60,48}, Shuai Liu⁴⁶, T. Liu^{1,52}, X. Liu³², Y. B. Liu³⁷, Z. A. Liu^{1,48,52}, Z. Q. Liu⁴¹, Y. F. Long^{38,k}, X. C. Lou^{1,48,52}, F. X. Lu¹⁶, H. J. Lu¹⁸, J. D. Lu^{1,52}, J. G. Lu^{1,48}, X. L. Lu¹, Y. Lu¹, Y. P. Lu^{1,48}, C. L. Luo³⁵, M. X. Luo⁶⁷, P. W. Luo⁴⁹, T. Luo^{9,h}, X. L. Luo^{1,48}, S. Lusso^{63C}, X. R. Lyu⁵², F. C. Ma³⁴, H. L. Ma¹, L. L. Ma⁴¹, M. M. Ma^{1,52}, Q. M. Ma¹, R. Q. Ma^{1,52}, R. T. Ma⁵², X. N. Ma³⁷, X. X. Ma^{1,52}, X. Y. Ma^{1,48}, Y. M. Ma⁴¹, F. E. Maas¹⁵, M. Maggiora^{63A,63C}, S. Maldaner²⁸, S. Malde⁵⁸, Q. A. Malik⁶², A. Mangoni^{23B}, Y. J. Mao^{38,k}, Z. P. Mao¹, S. Marcello^{63A,63C}, Z. X. Meng⁵⁴, J. G. Messchendorp³¹, G. Mezzadri^{24A}, T. J. Min³⁶, R. E. Mitchell²², X. H. Mo^{1,48,52}, Y. J. Mo⁶, N. Yu. Muchnoi^{10,c}, H. Muramatsu⁵⁶, S. Nakhoul^{11,f}, Y. Nefedov²⁹, F. Nerling^{11,f}, I. B. Nikolaev^{10,c}, Z. Ning^{1,48}, S. S. Nisar^{8,i}, S. L. Olsen⁵², Q. Ouyang^{1,48,52}, S. Pacetti^{23B,23C}, X. Pan^{9,h}, Y. Pan⁵⁵, A. Pathak¹, P. Patteri^{23A}, M. Pelizaeus⁴, H. P. Peng^{60,48}, S. H. Peters^{11,f}, J. Pettersson⁶⁴, J. L. Ping³⁵, R. G. Ping^{1,52}, A. Pitka⁴, R. Poling⁵⁶, V. Prasad^{60,48}, H. Qi^{60,48}, H. R. Qi⁵⁰, M. Qi³⁶, T. Y. Qi², T. Y. Qi⁹, S. Qian^{1,48}, W.-B. Qian⁵², Z. Qian⁴⁹, C. F. Qiao⁵², L. Q. Qin¹², X. S. Qin⁴, Z. H. Qin^{1,48}, J. F. Qiu¹, S. Q. Qu³⁷, K. H. Rashid⁶², K. Ravindran²¹, C. F. Redmer²⁸, A. Rivetti^{63C}, V. Rodin³¹, M. Rolo^{63C}, G. Rong^{1,52}, Ch. Rosner¹⁵, M. Rump⁵⁷, A. Sarantsev^{29,d}, Y. Schelhaas²⁸, C. Schmier⁴, K. Schoenning⁶⁴, M. Scodeggio^{24A}, D. C. Shan⁴⁶, W. Shan¹⁹, X. Y. Shan^{60,48}, M. Shao^{60,48}, C. P. Shen⁹, P. X. Shen³⁷, X. Y. Shen^{1,52}, H. C. Shi^{60,48}, R. S. Shi^{1,52}, X. Shi^{1,48}, X. D. Shi^{60,48}, J. J. Song⁴¹, Q. Q. Song^{60,48}, W. M. Song^{27,1}, Y. X. Song^{38,k}, S. Sosio^{63A,63C}, S. Spataro^{63A,63C}, F. F. Sui⁴¹, G. X. Sun¹, J. F. Sun¹⁶, L. Sun⁶⁵, S. S. Sun^{1,52}, T. Sun^{1,52}, W. Y. Sun³⁵, X. Sun^{20,l}, Y. J. Sun^{60,48}, Y. K. Sun^{60,48}, Y. Z. Sun¹, Z. T. Sun¹, Y. H. Tan⁶⁵, Y. X. Tan^{60,48}, C. J. Tang⁴⁵, G. Y. Tang¹, J. Tang⁴⁹, V. Thoren⁶⁴, I. Uman^{51D}, B. Wang¹, B. L. Wang⁵², C. W. Wang³⁶, D. Y. Wang^{38,k}, H. P. Wang^{1,52}, K. Wang^{1,48}, L. L. Wang¹, M. Wang⁴¹, M. Z. Wang^{38,k}, Meng Wang^{1,52}, W. H. Wang⁶⁵, W. P. Wang^{60,48}, X. Wang^{38,k}, X. F. Wang³², X. L. Wang^{9,h}, Y. Wang^{60,48}, Y. Wang⁴⁹, Y. D. Wang¹⁵, Y. F. Wang^{1,48,52}, Y. Q. Wang¹, Z. Wang^{1,48}, Z. Y. Wang¹, Ziyi Wang⁵², Zongyuan Wang^{1,52}, D. H. Wei¹², P. Weidenkaff²⁸, F. Weidner⁵⁷, S. P. Wen¹, D. J. White⁵⁵, U. Wiedner⁴, G. Wilkinson⁵⁸, M. Wolke⁶⁴, L. Wollenberg⁴, J. F. Wu^{1,52}, L. H. Wu¹, L. J. Wu^{1,52}, X. Wu^{9,h}, Z. Wu^{1,48}, L. Xia^{60,48}, H. Xiao^{9,h}, S. Y. Xiao¹, Y. J. Xiao^{1,52}, Z. J. Xiao³⁵, X. H. Xie^{38,k}, Y. G. Xie^{1,48}, Y. H. Xie⁶, T. Y. Xing^{1,52}, X. A. Xiong^{1,52}, G. F. Xu¹, J. J. Xu³⁶, Q. J. Xu¹⁴, W. Xu^{1,52}, X. P. Xu⁴⁶, F. Yan^{9,h}, L. Yan^{9,h}, L. Yan^{63A,63C}, W. B. Yan^{60,48}, W. C. Yan⁶⁸, Xu Yan⁴⁶, H. J. Yang^{42,g}, H. X. Yang¹, L. Yang⁶⁵, R. X. Yang^{60,48}, S. L. Yang^{1,52}, Y. H. Yang³⁶, Y. X. Yang¹², Yifan Yang^{1,52}, Zhi Yang²⁵, M. Ye^{1,48}, M. H. Ye⁷, J. H. Yin¹, Z. Y. You⁴⁹, B. X. Yu^{1,48,52}, C. X. Yu³⁷, G. Yu^{1,52}, J. S. Yu^{20,l}, T. Yu⁶¹, C. Z. Yuan^{1,52}, W. Yuan^{63A,63C}, X. Q. Yuan^{38,k}, Y. Yuan¹, Z. Y. Yuan⁴⁹, C. X. Yue³³, A. Yuncu^{51B,a}, A. A. Zafar⁶², Y. Zeng^{20,l}, B. X. Zhang¹, Guangyi Zhang¹⁶, H. H. Zhang⁴⁹, H. Y. Zhang^{1,48}, J. L. Zhang⁶⁶, J. Q. Zhang⁴, J. W. Zhang^{1,48,52}, J. Y. Zhang¹, J. Z. Zhang^{1,52}, Jianyu Zhang^{1,52}, Jiawei Zhang^{1,52}, L. Zhang¹, Lei Zhang³⁶, S. Zhang⁴⁹, S. F. Zhang³⁶, T. J. Zhang^{42,g}, X. Y. Zhang⁴¹, Y. Zhang⁵⁸, Y. H. Zhang^{1,48}, Y. T. Zhang^{60,48}, Yan Zhang^{60,48}, Yao Zhang¹, Yi Zhang^{9,h}, Z. H. Zhang⁶, Z. Y. Zhang⁶⁵, G. Zhao¹, J. Zhao³³, J. Y. Zhao^{1,52}, J. Z. Zhao^{1,48},

Lei Zhao^{60,48}, Ling Zhao¹, M. G. Zhao³⁷, Q. Zhao¹, S. J. Zhao⁶⁸, Y. B. Zhao^{1,48}, Y. X. Zhao²⁵, Z. G. Zhao^{60,48},
A. Zhemchugov^{29,b}, B. Zheng⁶¹, J. P. Zheng^{1,48}, Y. Zheng^{38,k}, Y. H. Zheng⁵², B. Zhong³⁵, C. Zhong⁶¹, L. P. Zhou^{1,52},
Q. Zhou^{1,52}, X. Zhou⁶⁵, X. K. Zhou⁵², X. R. Zhou^{60,48}, A. N. Zhu^{1,52}, J. Zhu³⁷, K. Zhu¹, K. J. Zhu^{1,48,52}, S. H. Zhu⁵⁹,
W. J. Zhu³⁷, X. L. Zhu⁵⁰, Y. C. Zhu^{60,48}, Z. A. Zhu^{1,52}, B. S. Zou¹, J. H. Zou¹

(BESIII Collaboration)

- ¹ Institute of High Energy Physics, Beijing 100049, People's Republic of China
² Beihang University, Beijing 100191, People's Republic of China
³ Beijing Institute of Petrochemical Technology, Beijing 102617, People's Republic of China
⁴ Bochum Ruhr-University, D-44780 Bochum, Germany
⁵ Carnegie Mellon University, Pittsburgh, Pennsylvania 15213, USA
⁶ Central China Normal University, Wuhan 430079, People's Republic of China
⁷ China Center of Advanced Science and Technology, Beijing 100190, People's Republic of China
⁸ COMSATS University Islamabad, Lahore Campus, Defence Road, Off Raiwind Road, 54000 Lahore, Pakistan
⁹ Fudan University, Shanghai 200443, People's Republic of China
¹⁰ G.I. Budker Institute of Nuclear Physics SB RAS (BINP), Novosibirsk 630090, Russia
¹¹ GSI Helmholtzcentre for Heavy Ion Research GmbH, D-64291 Darmstadt, Germany
¹² Guangxi Normal University, Guilin 541004, People's Republic of China
¹³ Guangxi University, Nanning 530004, People's Republic of China
¹⁴ Hangzhou Normal University, Hangzhou 310036, People's Republic of China
¹⁵ Helmholtz Institute Mainz, Johann-Joachim-Becher-Weg 45, D-55099 Mainz, Germany
¹⁶ Henan Normal University, Xinxiang 453007, People's Republic of China
¹⁷ Henan University of Science and Technology, Luoyang 471003, People's Republic of China
¹⁸ Huangshan College, Huangshan 245000, People's Republic of China
¹⁹ Hunan Normal University, Changsha 410081, People's Republic of China
²⁰ Hunan University, Changsha 410082, People's Republic of China
²¹ Indian Institute of Technology Madras, Chennai 600036, India
²² Indiana University, Bloomington, Indiana 47405, USA
²³ (A)INFN Laboratori Nazionali di Frascati, I-00044, Frascati, Italy; (B)INFN Sezione di Perugia, I-06100, Perugia, Italy;
(C)University of Perugia, I-06100, Perugia, Italy
²⁴ (A)INFN Sezione di Ferrara, I-44122, Ferrara, Italy; (B)University of Ferrara, I-44122, Ferrara, Italy
²⁵ Institute of Modern Physics, Lanzhou 730000, People's Republic of China
²⁶ Institute of Physics and Technology, Peace Ave. 54B, Ulaanbaatar 13330, Mongolia
²⁷ Jilin University, Changchun 130012, People's Republic of China
²⁸ Johannes Gutenberg University of Mainz, Johann-Joachim-Becher-Weg 45, D-55099 Mainz, Germany
²⁹ Joint Institute for Nuclear Research, 141980 Dubna, Moscow region, Russia
³⁰ Justus-Liebig-Universitaet Giessen, II. Physikalisches Institut, Heinrich-Buff-Ring 16, D-35392 Giessen, Germany
³¹ KVI-CART, University of Groningen, NL-9747 AA Groningen, The Netherlands
³² Lanzhou University, Lanzhou 730000, People's Republic of China
³³ Liaoning Normal University, Dalian 116029, People's Republic of China
³⁴ Liaoning University, Shenyang 110036, People's Republic of China
³⁵ Nanjing Normal University, Nanjing 210023, People's Republic of China
³⁶ Nanjing University, Nanjing 210093, People's Republic of China
³⁷ Nankai University, Tianjin 300071, People's Republic of China
³⁸ Peking University, Beijing 100871, People's Republic of China
³⁹ Qufu Normal University, Qufu 273165, People's Republic of China
⁴⁰ Shandong Normal University, Jinan 250014, People's Republic of China
⁴¹ Shandong University, Jinan 250100, People's Republic of China
⁴² Shanghai Jiao Tong University, Shanghai 200240, People's Republic of China
⁴³ Shanxi Normal University, Linfen 041004, People's Republic of China
⁴⁴ Shanxi University, Taiyuan 030006, People's Republic of China
⁴⁵ Sichuan University, Chengdu 610064, People's Republic of China
⁴⁶ Soochow University, Suzhou 215006, People's Republic of China
⁴⁷ Southeast University, Nanjing 211100, People's Republic of China
⁴⁸ State Key Laboratory of Particle Detection and Electronics, Beijing 100049, Hefei 230026, People's Republic of China
⁴⁹ Sun Yat-Sen University, Guangzhou 510275, People's Republic of China

- ⁵⁰ Tsinghua University, Beijing 100084, People's Republic of China
- ⁵¹ (A)Ankara University, 06100 Tandogan, Ankara, Turkey; (B)Istanbul Bilgi University, 34060 Eyup, Istanbul, Turkey; (C)Uludag University, 16059 Bursa, Turkey; (D)Near East University, Nicosia, North Cyprus, Mersin 10, Turkey
- ⁵² University of Chinese Academy of Sciences, Beijing 100049, People's Republic of China
- ⁵³ University of Hawaii, Honolulu, Hawaii 96822, USA
- ⁵⁴ University of Jinan, Jinan 250022, People's Republic of China
- ⁵⁵ University of Manchester, Oxford Road, Manchester, M13 9PL, United Kingdom
- ⁵⁶ University of Minnesota, Minneapolis, Minnesota 55455, USA
- ⁵⁷ University of Muenster, Wilhelm-Klemm-Str. 9, 48149 Muenster, Germany
- ⁵⁸ University of Oxford, Keble Rd, Oxford, UK OX13RH
- ⁵⁹ University of Science and Technology Liaoning, Anshan 114051, People's Republic of China
- ⁶⁰ University of Science and Technology of China, Hefei 230026, People's Republic of China
- ⁶¹ University of South China, Hengyang 421001, People's Republic of China
- ⁶² University of the Punjab, Lahore-54590, Pakistan
- ⁶³ (A)University of Turin, I-10125, Turin, Italy; (B)University of Eastern Piedmont, I-15121, Alessandria, Italy; (C)INFN, I-10125, Turin, Italy
- ⁶⁴ Uppsala University, Box 516, SE-75120 Uppsala, Sweden
- ⁶⁵ Wuhan University, Wuhan 430072, People's Republic of China
- ⁶⁶ Xinyang Normal University, Xinyang 464000, People's Republic of China
- ⁶⁷ Zhejiang University, Hangzhou 310027, People's Republic of China
- ⁶⁸ Zhengzhou University, Zhengzhou 450001, People's Republic of China
- ^a Also at Bogazici University, 34342 Istanbul, Turkey
- ^b Also at the Moscow Institute of Physics and Technology, Moscow 141700, Russia
- ^c Also at the Novosibirsk State University, Novosibirsk, 630090, Russia
- ^d Also at the NRC "Kurchatov Institute", PNPI, 188300, Gatchina, Russia
- ^e Also at Istanbul Arel University, 34295 Istanbul, Turkey
- ^f Also at Goethe University Frankfurt, 60323 Frankfurt am Main, Germany
- ^g Also at Key Laboratory for Particle Physics, Astrophysics and Cosmology, Ministry of Education; Shanghai Key Laboratory for Particle Physics and Cosmology; Institute of Nuclear and Particle Physics, Shanghai 200240, People's Republic of China
- ^h Also at Key Laboratory of Nuclear Physics and Ion-beam Application (MOE) and Institute of Modern Physics, Fudan University, Shanghai 200443, People's Republic of China
- ⁱ Also at Harvard University, Department of Physics, Cambridge, MA, 02138, USA
- ^j Currently at: Institute of Physics and Technology, Peace Ave.54B, Ulaanbaatar 13330, Mongolia
- ^k Also at State Key Laboratory of Nuclear Physics and Technology, Peking University, Beijing 100871, People's Republic of China
- ^l School of Physics and Electronics, Hunan University, Changsha 410082, China

Abstract

Based on 586 pb^{-1} of e^+e^- annihilation data collected at a center-of-mass energy of $\sqrt{s} = 4.6 \text{ GeV}$ with the BESIII detector at the BEPCII collider, the absolute branching fraction of $\Lambda_c^+ \rightarrow pK_S^0\eta$ decays is measured for the first time to be $\mathcal{B}(\Lambda_c^+ \rightarrow pK_S^0\eta) = (0.414 \pm 0.084 \pm 0.028)\%$, where the first uncertainty is statistical and the second is systematic. The result is compatible with a previous CLEO result on the relative branching fraction $\frac{\mathcal{B}(\Lambda_c^+ \rightarrow pK_S^0\eta)}{\mathcal{B}(\Lambda_c^+ \rightarrow pK^-\pi^+)}$, and consistent with theoretical predictions of SU(3) flavor symmetry.

Keywords: charmed baryon, Λ_c^+ decays, absolute branching fraction, BESIII

1. Introduction

The lightest charmed baryon, Λ_c^+ , was first observed in the 1970s [1, 2], but only in the past few years has there been significant progress in precision measurements of its absolute decay rates [3, 4]. Driven by these improvements, the theoretical calculations of charmed baryon decays have greatly improved their treatment of non-perturbative effects [5–8]. However, more experimental and theoretical efforts are needed to further improve the understanding of non-factorizable effects, which are non-trivial in the charmed baryon sector [7, 9]. More experimental data are also desired to test existing theoretical predictions [10].

The hadronic decay $\Lambda_c^+ \rightarrow pK_S^0\eta$ offers important information about the dynamics of charmed baryon decays [11]. The charge-conjugate mode is always implied throughout this Letter. The branching fraction (BF) $\mathcal{B}(\Lambda_c^+ \rightarrow pK_S^0\eta) = \mathcal{B}(\Lambda_c^+ \rightarrow p\bar{K}^0\eta)/2 = (0.8 \pm 0.2)\%$ has only been measured relative to $\Lambda_c^+ \rightarrow pK^-\pi^+$ [12]. However, recent comprehensive theoretical analyses of different BFs for Λ_c^+ decays to three-body final states, which assume SU(3) flavor symmetry, predict that $\mathcal{B}(\Lambda_c^+ \rightarrow pK_S^0\eta)$ is in the range 0.35% to 0.45% [11, 14]. There is a discrepancy of approximately 2 standard deviations between the existing experimental result and those new theoretical calculations. Further, $\Lambda_c^+ \rightarrow pK_S^0\eta$ is regarded as an important channel to understand the properties of the intermediate $N(1535)$ resonance [15, 16]. The $N(1535)$ resonance is puzzling because it decays to final states that contain strange hadrons, like ηN and $K\Lambda$ [13, 15, 16], but it does not contain any $\bar{s}s$ component according to the naive constituent quark model. Thus, further measurements of the $\Lambda_c^+ \rightarrow pK_S^0\eta$ decays may help to verify SU(3) flavor symmetry and may reveal the intermediate states contributing to these decays.

In this Letter, we present the first absolute measurement of the BF for $\Lambda_c^+ \rightarrow pK_S^0\eta$ decays based on an e^+e^- collision data sample corresponding to an integrated luminosity of 586 pb^{-1} , collected at the center-of-mass energy of $\sqrt{s} = 4.6 \text{ GeV}$ with the BESIII detector [17] at the Beijing Electron Positron Collider (BEPCII) [18]. At this energy, the Λ_c^+ baryon is always produced along with a $\bar{\Lambda}_c^-$, and the energy remaining does not allow the production of any additional hadrons. In this analysis, we use the single tag (ST) method in which the $\Lambda_c^+ \rightarrow pK_S^0\eta$ is reconstructed while the $\bar{\Lambda}_c^-$ is not.

2. BESIII Detector and Monte Carlo Simulation

The BESIII detector is a magnetic spectrometer [17] located at BEPCII [18]. The cylindrical core of the BESIII detector consists of a helium-based multilayer drift chamber (MDC), a plastic scintillator time-of-flight system (TOF), and a CsI(Tl) electromagnetic calorimeter (EMC), which are all enclosed in a superconducting solenoidal magnet providing a 1.0 T magnetic field. The solenoid is supported by an octagonal flux-return yoke with resistive-plate-counter muon-identifier modules interleaved with steel. The acceptance of charged particles and photons is 93% of the 4π solid angle. The charged-particle momentum resolution at 1 GeV/c is 0.5%, and the dE/dx resolution is 6% for electrons from Bhabha scattering. The EMC measures photon energies with a resolution of 2.5% (5%) at 1 GeV in the barrel (end cap) region. The time resolution of the TOF barrel part is 68 ps, while that of the end cap part is 110 ps.

Samples of simulated events produced with the GEANT4-based [19] Monte Carlo (MC) package which includes the geometric description of the BESIII detector and the detector response, are used to determine the detection efficiency and estimate the backgrounds. The simulation includes the beam energy spread and initial state radiation (ISR) in the e^+e^- annihilations modeled with the generator KKMC [20]. Two types of MC samples are generated in this analysis. The signal MC samples, in which the Λ_c^+ decays non-resonantly to $\Lambda_c^+ \rightarrow pK_S^0\eta$ while the $\bar{\Lambda}_c^-$ decays into all possible channels, are used to determine the detection efficiency. The inclusive MC sample, which consists of the production of $\Lambda_c^+\bar{\Lambda}_c^-$ pairs and open-charm mesons, the ISR production of vector charmonium(-like) states, and the continuum processes incorporated in KKMC [20], is used to estimate the backgrounds. Known decay modes are modeled with EVTGEN [21] using BFs taken from the PDG [13], and the remaining unknown decays from the charmonium states are modeled with LUNDCHARM [22]. The final-state radiation from charged final-state particles is incorporated using the PHOTOS package [23].

3. Event selection

In this analysis, all the charged tracks are required to satisfy $|\cos\theta| < 0.93$, where θ is the polar angle of the charged track with respect to the axis of the MDC. For the proton, the distance of closest approach to the interaction point (IP) must be within $\pm 10 \text{ cm}$ along the

MDC axis (V_z) and within ± 1 cm in the plane perpendicular to the MDC axis (V_r). The particle identification (PID) algorithm combines the dE/dx information from the MDC and flight time from the TOF to evaluate the likelihood $\mathcal{L}(h)(h = \pi, K, p)$ for the different final state hadron hypotheses; to be classified as a proton we require the charged track satisfies both $\mathcal{L}(p) > \mathcal{L}(\pi)$ and $\mathcal{L}(p) > \mathcal{L}(K)$.

We reconstruct $K_S^0 \rightarrow \pi^+\pi^-$ candidates by combining two oppositely charged tracks. For these tracks, the distance of closest approach to the IP must be within ± 20 cm along the MDC axis. No requirement on either V_r or the PID likelihood is applied to maximize the efficiency. The two tracks are constrained to a common decay vertex by applying a vertex fit, and the corresponding χ^2 is required to be less than 100. The momenta of the $\pi^+\pi^-$ pairs corrected by the vertex fit are used in the following analysis. Further, the distance of the decay vertex of the K_S^0 from the IP is required to be larger than twice the estimated resolution. The invariant mass of the $\pi^+\pi^-$ pairs, $M_{\pi^+\pi^-}$, is required to lie in the mass region $(0.487, 0.511)$ GeV/ c^2 .

The η candidates are formed by photon pairs with their invariant mass satisfying the requirement 0.500 GeV/ $c^2 < M_{\gamma\gamma} < 0.565$ GeV/ c^2 . Here, the γ candidates are reconstructed from clusters in the EMC crystals that are not matched with any charged tracks. The energy deposited in the nearby time-of-flight counters is included in the photon reconstruction. The deposited energy of any cluster is required to be larger than 25 MeV in the barrel region ($|\cos\theta| < 0.8$) or 50 MeV in the end cap region ($0.86 < |\cos\theta| < 0.92$). The measured EMC time of the cluster, which is defined as the shower time recorded by the EMC relative to the event start time, is required to be within $(0, 700)$ ns to suppress electronic noise and energy deposits unrelated to the event. A kinematic fit is applied to constrain $M_{\gamma\gamma}$ to the nominal mass of the η meson [13]. The momenta of the $\gamma\gamma$ pairs corrected by the kinematic fit are used for further analysis.

The Λ_c^+ candidates are formed by all combinations of proton, K_S^0 and η candidates in an event. Two kinematic variables, the energy difference $\Delta E \equiv E_{\Lambda_c^+} - E_{\text{beam}}$ and the beam-constrained mass $M_{\text{BC}} \equiv \sqrt{E_{\text{beam}}^2/c^4 - |\vec{p}_{\Lambda_c^+}|^2/c^2}$, are defined to identify Λ_c^+ candidates. Here, $E_{\Lambda_c^+}$ and $\vec{p}_{\Lambda_c^+}$ are the reconstructed energy and momentum of the Λ_c^+ candidates calculated in the e^+e^- rest frame, and E_{beam} is the average energy of the e^+ and e^- beams. All the candidates are required to satisfy -0.07 GeV $< \Delta E < 0.07$ GeV and 2.25 GeV/ $c^2 < M_{\text{BC}} < 2.3$ GeV/ c^2 . If more than

one candidate in an event satisfies all the above requirements, the best candidate is selected with the following sequence. First, we select candidates that contain the proton with the largest $\mathcal{L}(p)$. Second, if there are still multiple candidates, we select those that contain the K_S^0 with the largest decay length in units of its resolution. Finally, if there are still multiple candidates after the proton and K_S^0 requirements, we select the candidate that contains the η with the smallest χ^2 returned by the kinematic fit. About 16.9% of total events in data have multiple candidates, and the probability to select the correct candidate is 63.1% based on a MC study.

4. Signal yield and BF

To determine the signal yield of $\Lambda_c^+ \rightarrow pK_S^0\eta$, an unbinned maximum likelihood fit is performed on the two-dimensional distribution of M_{BC} versus ΔE . Based on the K_S^0 sideband (0.02 GeV/ $c^2 < |m(\pi^+\pi^-) - m(K_S^0)| < 0.03$ GeV/ c^2) from data, and inclusive MC studies, no peaking background is found in either the M_{BC} or ΔE signal region. In the fit, the M_{BC} and ΔE background shapes are modeled by an ARGUS function [24] and a second-order Chebyshev polynomial function, respectively. The M_{BC} and ΔE background shapes are treated as uncorrelated based on MC validation. The signal shape is the MC-derived two-dimensional shape convolved with Gaussian functions in each dimension, where the Gaussian functions compensate for the resolution difference between data and MC samples. The parameters of the Gaussian functions for ΔE and M_{BC} are fixed to the values determined from the corresponding one-dimensional fits in data.

Figure 1 shows the one-dimensional projection plots of the fit results. The signal yield is obtained to be $N_{\text{sig}} = 42.0 \pm 8.5$, where the uncertainty is statistical only. The statistical significance for the signal is 7.3σ , which is evaluated by the change of the likelihood between the nominal fit and the fit without the signal component. The detection efficiency, which is estimated by using the signal MC sample, is $\varepsilon = (17.57 \pm 0.01)\%$. Thus, the absolute BF of $\Lambda_c^+ \rightarrow pK_S^0\eta$ can be obtained by

$$\mathcal{B}(\Lambda_c^+ \rightarrow pK_S^0\eta) = \frac{N_{\text{sig}}}{2 \cdot N_{\Lambda_c^+\bar{\Lambda}_c^-} \cdot \mathcal{B}_{\text{inter}} \cdot \varepsilon}, \quad (1)$$

where $\mathcal{B}_{\text{inter}} = \mathcal{B}(K_S^0 \rightarrow \pi^+\pi^-) \cdot \mathcal{B}(\eta \rightarrow \gamma\gamma)$ is the product of the BFs of the intermediate states taken from the PDG [13], and $N_{\Lambda_c^+\bar{\Lambda}_c^-} = (105.9 \pm 5.3) \times 10^3$ is the total number of $\Lambda_c^+\bar{\Lambda}_c^-$ pairs in data [25]. Using Eq. 1, we calculate $\mathcal{B}(\Lambda_c^+ \rightarrow pK_S^0\eta) = (0.414 \pm 0.084)\%$, where the uncertainty is statistical only.

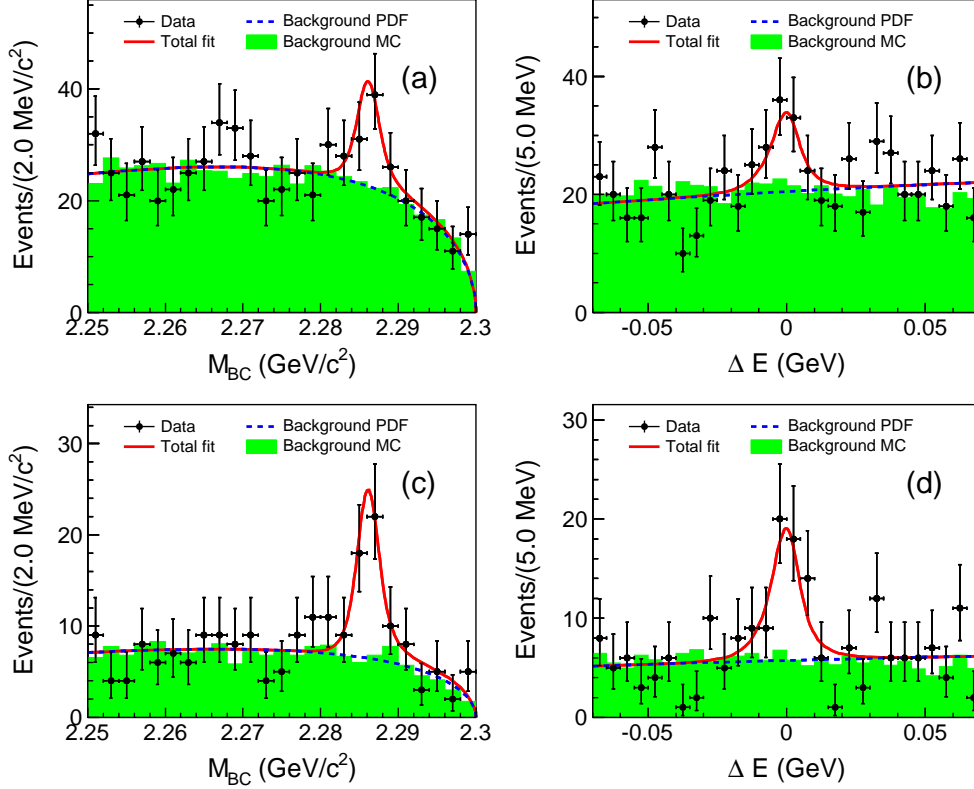


Figure 1: One-dimensional projection plots of (a) M_{BC} and (b) ΔE distributions, as well as background reduced projection plots of (c) M_{BC} ($|\Delta E| < 0.02$ GeV) and (d) ΔE (2.28 GeV/ $c^2 < M_{BC} < 2.295$ GeV/ c^2) with the fit results. Points with error bars are data, the solid red line is the total fit result, the blue-dashed line is the background contribution, and the green histogram is the background distribution from the inclusive MC sample.

5. Systematic uncertainties

In this work, the systematic uncertainties on the BF measurement include the uncertainties related to the PID and tracking of the proton, the reconstruction of the K_S^0 and η , the two-dimensional fit, the MC modeling, $N_{\Lambda_c^+ \bar{\Lambda}_c^-}$ and the BFs of the intermediate states.

The uncertainties related to the PID and tracking of the proton are estimated to be 1%, respectively, based on a study of control samples of $e^+e^- \rightarrow p\bar{p}\pi^+\pi^-$ and $e^+e^- \rightarrow p\bar{p}\pi^+\pi^-\pi^+\pi^-$ events in data at $\sqrt{s} > 4.23$ GeV [25]. The uncertainty associated with the K_S^0 reconstruction is assigned to be 2.5% based on studies of control samples of $J/\psi \rightarrow K^*(892)^\mp K^\pm$ and $J/\psi \rightarrow \phi K_S^0 K^\mp \pi^\pm$ decays [25]. We use a control sample of $D^0 \rightarrow K^-\pi^+\pi^0$ events to estimate the uncertainty due to the η reconstruction [26, 27]. The $\pi^0 \rightarrow \gamma\gamma$ reconstruction efficiencies are obtained in data and MC simulations, and an η reconstruction uncertainty of 1.8% is assigned by weighting the efficiency difference to the η momentum distribution of the signal

samples.

The uncertainty associated with the two-dimensional fit consists of the uncertainties of the signal and background shapes. To estimate the uncertainty, 20000 pseudo-data-sets are sampled with replacement data according to the bootstrap method [28]. For each pseudo-data-set, a two-dimensional fit is performed, in which the mean values and standard deviations of the two Gaussian functions in the signal shape are randomly varied by $\pm 1\sigma$ around their nominal values, and the endpoint of the ARGUS function is randomly varied by ± 0.2 MeV around its nominal value. The pull of the fit result $p(N_{\text{sig}})$ is defined as

$$p(N_{\text{sig}}) = \frac{N_{\text{sig}}^{\text{pseudo}} - N_{\text{sig}}^{\text{real}}}{\sigma_N^{\text{pseudo}}}, \quad (2)$$

where $N_{\text{sig}}^{\text{real}}$ is the fit yield of real data, $N_{\text{sig}}^{\text{pseudo}}$ and σ_N^{pseudo} are the fit yield and its statistical uncertainty of the pseudo-data, respectively. The distribution of

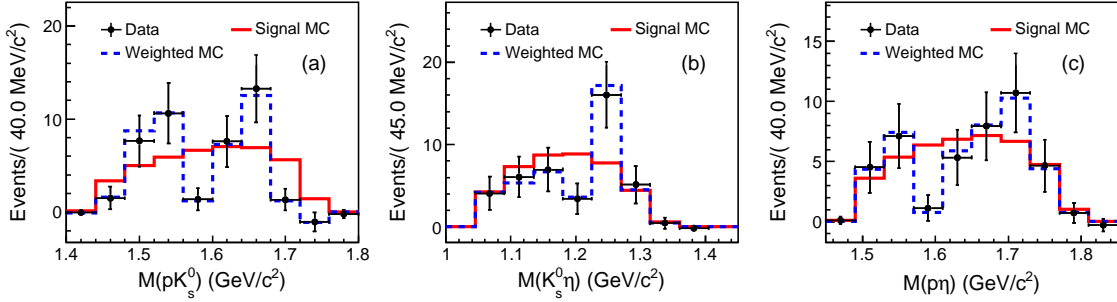


Figure 2: Distributions of (a) $M_{pK_S^0}$, (b) $M_{K_S^0\eta}$ and (c) $M_{p\eta}$ in data and signal MC samples, in which points with error bars are data after the background subtraction, and the red-solid and blue-dashed histograms show the unweighted and weighted signal MC samples, respectively.

$p(N_{\text{sig}})$ values is fitted with a Gaussian function, and the mean value is obtained to be -0.1364 ± 0.0074 . The bias in $p(N_{\text{sig}})$ is 13.64% of the statistical uncertainty, which is calculated to be 2.8%, and as no correction for this bias is applied, we use 2.8% as the systematic uncertainty related with the two-dimensional fit.

The uncertainty related to the MC model of the signal process is evaluated by reweighting the signal MC sample, which is generated assuming no intermediate resonances, according to the $M_{pK_S^0}$, $M_{K_S^0\eta}$ and $M_{p\eta}$ invariant mass distributions observed in data. Here, M_{ij} is the invariant mass of the combination of particles i and j . Figure 2 shows the distributions of these invariant masses in data after the background subtraction using the *sPlot* method [29]. The detection efficiency based on the modified MC sample is calculated to be 17.19%, and the relative difference to the nominal efficiency, 2.2%, is taken as the corresponding systematic uncertainty.

The uncertainty of $N_{\Lambda_c^+ \bar{\Lambda}_c^-}$ in data is reported to be 4.6% in Ref. [25]. The BFs of intermediate states from the PDG [13] are $\mathcal{B}(K_S^0 \rightarrow \pi^+ \pi^-) = (69.20 \pm 0.05)\%$ and $\mathcal{B}(\eta \rightarrow \gamma\gamma) = (39.41 \pm 0.20)\%$. The uncertainty from these two BFs, which is dominated by the latter one, is 0.5%.

The total systematic uncertainty, which is determined by adding all sources of systematic uncertainties in quadrature, is calculated to be 6.8%. The systematic uncertainties are summarized in Table 1.

Table 1: Systematic uncertainties.

Source	Uncertainty (%)
Proton PID	1.0
Proton Tracking	1.0
K_S^0 reconstruction	2.5
η reconstruction	1.8
Two-dimensional fit	2.8
Signal model	2.2
$N_{\Lambda_c^+ \bar{\Lambda}_c^-}$	4.6
$\mathcal{B}_{\text{inter}}$	0.5
Total	6.8

6. Summary

Based on 586 pb^{-1} of e^+e^- collision data collected at $\sqrt{s} = 4.6 \text{ GeV}$ with the BESIII detector and the BEPCII collider, the absolute BF for $\Lambda_c^+ \rightarrow pK_S^0\eta$ is determined for the first time. The BF is measured to be $\mathcal{B}(\Lambda_c^+ \rightarrow pK_S^0\eta) = (0.414 \pm 0.084 \pm 0.028)\%$, where the first uncertainty is statistical and the second one is systematic. The statistical significance of this decay is larger than 7σ . This result is compatible with the CLEO result $\mathcal{B}(\Lambda_c^+ \rightarrow pK_S^0\eta) = (0.8 \pm 0.2)\%$ [12] within 1.5σ . Our result is consistent with theoretical predictions based on SU(3) symmetry [11, 14]. With present statistics, it is not practical to measure any intermediate N^* states, as suggested in Refs. [15, 16].

7. Acknowledgments

The BESIII collaboration thanks the staff of BEPCII and the IHEP computing center for their strong support. This work is supported in part by National Key Basic Research Program of China under Contract No. 2015CB856700, 2020YFA0406300,

2020YFA0406400; National Natural Science Foundation of China (NSFC) under Contracts Nos. 11425524, 11575193, 11625523, 11635010, 11735014, 11822506, 11835012, 11935015, 11935016, 11935018, 11961141012, 11805086, U1732266; the Youth Innovation Promotion Association of CAS under Contract No. 2016153; the Chinese Academy of Sciences (CAS) Large-Scale Scientific Facility Program; Open Research Program of Large Research Infrastructures (2017), Chinese Academy of Sciences; Joint Large-Scale Scientific Facility Funds of the NSFC and CAS under Contracts Nos. U1732263, U1832207; CAS Key Research Program of Frontier Sciences under Contracts Nos. QYZDJ-SSW-SLH003, QYZDB-SSW-SLH039, QYZDJ-SSW-SLH040; 100 Talents Program of CAS; INPAC and Shanghai Key Laboratory for Particle Physics and Cosmology; ERC under Contract No. 758462; German Research Foundation DFG under Contracts Nos. 443159800, Collaborative Research Center CRC 1044, FOR 2359, GRK 214; Istituto Nazionale di Fisica Nucleare, Italy; Ministry of Development of Turkey under Contract No. DPT2006K-120470; National Science and Technology fund; Olle Engkvist Foundation under Contract No. 200-0605; STFC (United Kingdom); The Knut and Alice Wallenberg Foundation (Sweden) under Contract No. 2016.0157; The Royal Society, UK under Contracts Nos. DH140054, DH160214; The Swedish Research Council; U. S. Department of Energy under Contracts Nos. DE-FG02-05ER41374, DE-SC-0012069. This paper is also supported by the Fundamental Research Funds for the Central Universities of China.

References

- [1] B. Knapp *et al.*, Phys. Rev. Lett. **37**, 882 (1976).
- [2] G. S. Abrams *et al.* [Mark II Collaboration], Phys. Rev. Lett. **44**, 10 (1980).
- [3] D. M. Asner *et al.* [BESIII Collaboration], Int. J. Mod. Phys. A **24**, S1 (2009).
- [4] M. Ablikim *et al.* [BESIII Collaboration], Chin. Phys. C **44**, 040001 (2020).
- [5] H. Y. Cheng, Front. Phys. **10**, 101406 (2015).
- [6] C. D. Lü, W. Wang and F. S. Yu, Phys. Rev. D **93**, 056008 (2016).
- [7] H. Y. Cheng, X. W. Kang and F. Xu, Phys. Rev. D **97**, no.7, 074028 (2018).
- [8] C. Q. Geng, C. W. Liu and T. H. Tsai, Phys. Lett. B **790**, 225 (2019).
- [9] J. Zou, F. Xu, G. Meng and H. Y. Cheng, Phys. Rev. D **101**, no.1, 014011 (2020).
- [10] M. Gronau, J. L. Rosner and C. G. Wohl, Phys. Rev. D **97**, 116015 (2018).
- [11] C. Q. Geng, Y. K. Hsiao, C. W. Liu and T. H. Tsai, Phys. Rev. D **99**, 073003 (2019).
- [12] R. Ammar *et al.* [CLEO Collaboration], Phys. Rev. Lett. **74**, 3534 (1995).
- [13] P.A. Zyla *et al.* [Particle Data Group], to be published in Prog. Theor. Exp. Phys. 2020, 083C01 (2020).
- [14] J. Y. Cen, C. Q. Geng, C. W. Liu and T. H. Tsai, Eur. Phys. J. C **79**, 946 (2019).
- [15] J. J. Xie and L. S. Geng, Phys. Rev. D **96**, 054009 (2017).
- [16] R. Pavao, S. Sakai and E. Oset, Phys. Rev. C **98**, 015201 (2018).
- [17] M. Ablikim *et al.* [BESIII Collaboration], Nucl. Instrum. Meth. A **614**, 345 (2010).
- [18] C. H. Yu *et al.*, Proceedings of IPAC2016, Busan, Korea, 2016, doi:10.18429/JACoW-IPAC2016-TUYA01.
- [19] S. Agostinelli *et al.* [GEANT4 Collaboration], Nucl. Instrum. Meth. A **506**, 250 (2003).
- [20] S. Jadach, B. F. L. Ward and Z. Was, Phys. Rev. D **63**, 113009 (2001); Comput. Phys. Commun. **130**, 260 (2000).
- [21] D. J. Lange, Nucl. Instrum. Meth. A **462**, 152 (2001); R. G. Ping, Chin. Phys. C **32**, 599 (2008).
- [22] J. C. Chen, G. S. Huang, X. R. Qi, D. H. Zhang and Y. S. Zhu, Phys. Rev. D **62**, 034003 (2000); R. L. Yang, R. G. Ping and H. Chen, Chin. Phys. Lett. **31**, 061301 (2014).
- [23] E. Richter-Was, Phys. Lett. B **303**, 163 (1993).
- [24] H. Albrecht *et al.* [ARGUS Collaboration], Phys. Lett. B **241**, 278 (1990).
- [25] M. Ablikim *et al.* [BESIII Collaboration], Phys. Rev. Lett. **116**, 052001 (2016).
- [26] M. Ablikim *et al.* [BESIII Collaboration], Phys. Rev. D **96**, no.1, 012002 (2017).
- [27] M. Ablikim *et al.* [BESIII Collaboration], Phys. Rev. D **99**, no.3, 032010 (2019).
- [28] B. Efron, Annals Statist. **7**, 1 (1979).
- [29] M. Pivk and F. R. Le Diberder, Nucl. Instrum. Meth. A **555**, 356-369 (2005).